2024 IEEE International Conference on Robotics and Automation (ICRA 2024)
May 13-17, 2024. Yokohama, Japan

Iterative Learning Control for Deformable Open-Frame Cable-Driven Parallel Robots

Wuichung Cheng, Arthur Ngo Foon Chan, Darwin Lau

***Abstract*— This paper proposed an iterative learning control (ILC) scheme for deformable open-frame cable-driven parallel robots (D-CDPRs). In contrast to the straightforward inverse kinematics of the rigid frame cable-driven parallel robots (CDPRs), accurate modeling of the deformable frame poses challenges due to errors and uncertainties. To address these issues, the authors propose the use of ILC, a control strategy that modifies the control input over iterations based on previous results. ILC has been successfully applied to traditional cable robots, particularly in handling model uncertainty. The paper presents a novel ILC control scheme specifically designed for D-CDPRs, with a focus on reducing tracking errors over repetitive operations. Additionally, hardware experiments are conducted to validate the effectiveness and reliability of the proposed ILC approach. The results demonstrate the efficacy of ILC in mitigating tracking errors, even in scenarios where the dynamic model of the D-CDPRs is unknown.**

I. INTRODUCTION

Cable-driven parallel robots (CDPRs) are parallel manipulators that have flexible cables to maneuver the end effector (EE) [1]. Compared to traditional rigid links parallel robots, CDPRs have number of advantages such as larger workspaces, more favorable dynamic performance, higher payload-to-weight ratios, and more transportable [2], [3]. For CDPRs, the inverse kinematics is straightforward, where given the target EE pose, the required cable length could be calculated analytically. An assumption to attain this simple calculation is that the cable attachment points on the base frame are known. Hence the frames are usually built to be very rigid and heavy in order to resist the cable force during operation.

To further improve the portability and reduce the overall weight of the CDPR, we proposed in our previous work the deformable open-frame cable-driven parallel robots (D-CDPRs) [4], where the rigid frame of the CDPR is replaced by a deformable frame, as shown in Fig. 1. In contrast to traditional CDPR that always have stationary attachment points [5], [6], the D-CDPR's deforming frame results in spatially varying attachment points during robot operation. This frame deformation is caused by the cable forces that maneuver the EE.

To achieve the desire trajectory tracking performance, an accurate dynamic model of the deformable frame is essential. However, it is a challenging task as modeling errors always exist in reality. For example, a simplified beam model loses its accuracy in the case of large deflection. Second, some parameters are difficult to obtain experimentally, such as Young's modulus, moment of inertia, damping coefficient, and friction. Such model errors would ultimately result in tracking errors.

W. Cheng, A. N. F. Chan and D. Lau are with the Department of Mechanical and Automation Engineering, The Chinese University of Hong Kong, Hong Kong SAR. The work was supported by the Research Grants Council (General Research Fund Reference No. 14220822).

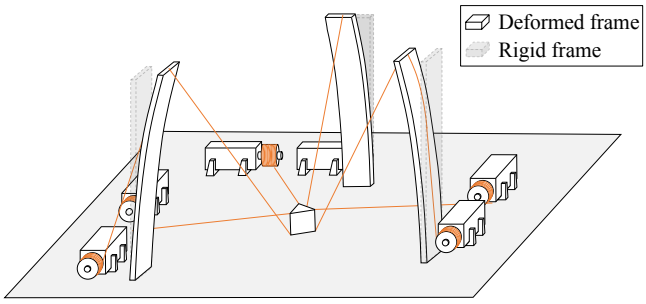

Fig. 1. Concept of deformable open-frame cable-driven parallel robots (D-CDPRs)

To tackle the error from the deformable frame, iterative learning control (ILC) can be considered to effectively reduce the tracking errors over iterations. ILC is specialized for improving the performance of repetitive operations [7]–[10]. By modifying the control input to the system over iterations using the result from the previous iterations [11]–[13], it has been applied to traditional cable robots to handle model uncertainty in the literature [14]–[16]. This control strategy is particularly useful for D-CDPRs when the dynamic model of the deformable frame is imperfect or unknown.

In this paper, an ILC control scheme is proposed and deployed for D-CDPRs. A novel Jacobian estimation approach specialized for deformable frames is proposed in section IV to improve the reliability and performance of the ILC law. A hardware experiment is conducted in section V to verify the proposed approaches. The results show that the proposed solution is effective and reliable in handling the tracking errors over repeating iterations.

II. KINEMATIC AND DYNAMIC MODEL OF D-CDPR

The frame of a D-CDPR is composed of m number of cantilever beams, which support the cable outlets (attachment points). Each beam has one cable attached to its tip independently. As shown in Fig. 2, the frame attachment point positions without beam deflection are known as constants $\hat{\boldsymbol{a}}_i \in \mathbb{R}^3$. During manipulation of the D-CDPR, the cable tensions deflect the tip of the cantilever to $\boldsymbol{a}_i(t)$. In this work, the cantilever is considered as an Euler-Bernoulli beam, which deflects under load perpendicularly to its neutral axis. Hence, it is assumed the deflection along the neutral axis is

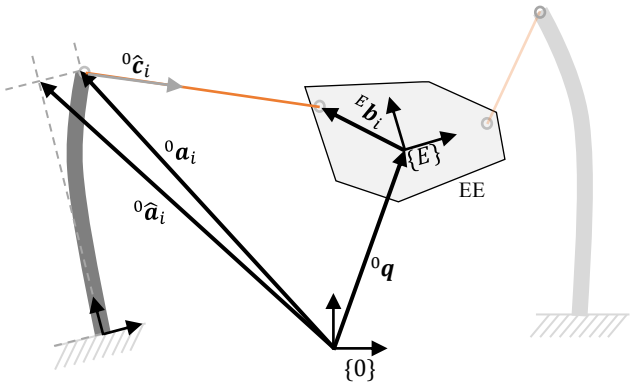

Fig. 2. Kinematics of a D-CDPR.

insignificant.

The pose of a generic 6-DoF EE, $\boldsymbol{q} \in \mathbb{R}^6$ is defined by its position $\boldsymbol{q}_p$ and orientation $\boldsymbol{q}_r$. Suppose the EE is actuated by m cables. The cable vector ${}^0\boldsymbol{c}_i$ is a vector of the ith cable that points from the frame attachment point ${}^0\boldsymbol{a}_i$ to the EE attachment points ${}^E\boldsymbol{b}_i$. The cable vector is given by

$$ {}^0\boldsymbol{c}_i = \boldsymbol{q}_p - {}^0\boldsymbol{a}_i + {}^0_E\boldsymbol{R}(\boldsymbol{q}_r)\,{}^E\boldsymbol{b}_i, \quad i = 1, ..., m \tag{1} $$

where the rotation matrix ${}^0_E\boldsymbol{R}$ is a function of orientation of the EE. Now define the cable length vector $\boldsymbol{l} \in \mathbb{R}^m$ as a collection of cable length of the CDPR. Mathematically, it is calculated by

$$ \boldsymbol{l} = \begin{bmatrix} \| {}^0\boldsymbol{c}_1 \|_2 \\ \vdots \\ \| {}^0\boldsymbol{c}_m \|_2 \end{bmatrix} = \begin{bmatrix} \sqrt{{}^0\boldsymbol{c}_1^T\,{}^0\boldsymbol{c}_1} \\ \vdots \\ \sqrt{{}^0\boldsymbol{c}_m^T\,{}^0\boldsymbol{c}_m} \end{bmatrix}. \tag{2} $$

Consider the time derivative of the cable length, one could obtain

$$ \dot{\boldsymbol{l}} = \begin{bmatrix} \frac{1}{l_1}({}^0\boldsymbol{c}_1^T\,{}^0\dot{\boldsymbol{c}}_1) \\ \vdots \\ \frac{1}{l_m}({}^0\boldsymbol{c}_m^T\,{}^0\dot{\boldsymbol{c}}_m) \end{bmatrix} = \begin{bmatrix} ({}^0\hat{\boldsymbol{c}}_1^T\,{}^0\dot{\boldsymbol{c}}_1) \\ \vdots \\ ({}^0\hat{\boldsymbol{c}}_m^T\,{}^0\dot{\boldsymbol{c}}_m) \end{bmatrix}, \tag{3} $$

where ${}^0\hat{\boldsymbol{c}}_i$ is the ith normal vector with $\| {}^0\hat{\boldsymbol{c}}_i \|_2 = 1$. Hence the cable speed vector is

$$ \dot{\boldsymbol{l}} = \begin{bmatrix} {}^0\hat{\boldsymbol{c}}_1^T\dot{\boldsymbol{q}}_p + {}^0\hat{\boldsymbol{c}}_1^T\boldsymbol{\omega} \times ({}^0_E\boldsymbol{R}\,{}^E\boldsymbol{b}_1) \\ \vdots \\ {}^0\hat{\boldsymbol{c}}_m^T\dot{\boldsymbol{q}}_p + {}^0\hat{\boldsymbol{c}}_m^T\boldsymbol{\omega} \times ({}^0_E\boldsymbol{R}\,{}^E\boldsymbol{b}_m) \end{bmatrix} = \boldsymbol{J}\dot{\boldsymbol{q}}, \tag{4} $$

where the EE's twist $\dot{\boldsymbol{q}} = [\dot{\boldsymbol{q}}_p^T,\ \boldsymbol{\omega}^T]^T$ is composed of linear and angular velocities w.r.t. $\{0\}$, respectively. The Jacobian matrix $\boldsymbol{J}$ transforms the cable speed (actuation) space to twist (task) space. The detailed deviation is given by

$$ \boldsymbol{J} = \begin{bmatrix} {}^0\hat{\boldsymbol{c}}_1{}^T & ({}^0_E\boldsymbol{R}\,{}^E\boldsymbol{b}_1 \times {}^0\hat{\boldsymbol{c}}_1)^T \\ \vdots & \vdots \\ {}^0\hat{\boldsymbol{c}}_m{}^T & ({}^0_E\boldsymbol{R}\,{}^E\boldsymbol{b}_m) \times {}^0\hat{\boldsymbol{c}}_m)^T \end{bmatrix}, \tag{5} $$

which depends on the normal cable vector ${}^0\hat{\boldsymbol{c}}_i$. On the other hand, the force equilibrium of the EE is described in the following equation,

$$ \boldsymbol{M}(\boldsymbol{q})\ddot{\boldsymbol{q}} + \boldsymbol{C}(\boldsymbol{q}, \dot{\boldsymbol{q}}) + \boldsymbol{g}(\boldsymbol{q}) + \boldsymbol{w}_{\text{ext}} = -\boldsymbol{J}^T(\boldsymbol{q}, \boldsymbol{A})\boldsymbol{\tau} \tag{6} $$

where $\boldsymbol{M} \in \mathbb{R}^{n \times n}$, $\boldsymbol{C} \in \mathbb{R}^n$, $\boldsymbol{g} \in \mathbb{R}^n$ and $\boldsymbol{w}_{ext} \in \mathbb{R}^n$ are the mass-inertia matrix, centrifugal and Coriolis vector, gravity vector, and external wrench vector, respectively. The attachment points are stored in a single vector $\boldsymbol{A} = [\boldsymbol{a}_1^T,\ \dots,\ \boldsymbol{a}_m^T]^T$.

III. Control Scheme

A. Length Control

The proposed D-CDPR is controlled by sending length commands to the motors simultaneously (Independent joint control or IJC) without real-time feedback of the EE pose or the beam deformation. This reduces the online signal transmission between the sensors and motors and thus simplifies the setup of the robot. In the experiment, the desired cable length is attained independently by a proportional–integral–derivative controller (PID). Hence the command current of each motor is calculated by

$$ I_i = k_p(l_i^r - l_i^a) + k_i \int (l_i^r - l_i^a)dt + k_d(\dot{l}_i^r - \dot{l}_i^a), \tag{7} $$

where $l_i^r,\ l_i^a,\ k_p,\ k_i,\ k_d$ are the reference (feedforward) cable length, actual (feedback) cable length, P gain, I gain and D gain respectively.

Compared to the tension control, which directly affects the EE acceleration, the length control is less sensitive to error and hence requires a lower operating frequency. The cable length has a direct relationship with the pose of the EE. As a result, many CDPRs can operate robustly using length control. Additionally, due to the simplicity of the inverse kinematics of the CDPR, the open-loop cable length command can be computed from equations (1) and (2). This control scheme is based on the assumption that the attachments of the frame are stationary.

However, this assumption does not hold when the frame is deformed by the cable tension. As the tension information is absent in the cable length controller, the frame deflection cannot be inferred. With the attachment locations $\boldsymbol{a}_i$ changing with the cable tension, the robot could not be accurately controlled using the fixed attachment locations assumption. Without a frame deflection model, conventional Jacobian based on fixed attachments are used to estimate the robot's kinematics. From the tracking results shown in the later experiment section, unsatisfactory tracking results are obtained. Those results are shown as the iteration 0 of the experiments in section V.

B. Gaussian Filter

A limitation of ILC is that it is difficult to handle non-repeating and chaotic disturbances. Such disturbance is mainly caused by sensor noise, background noise, and high order dynamics of the deformable frame. Feeding the measured EE pose directly to the ILC law would reduce the inter-iteration transient performance, or even cause divergence of tracking error.

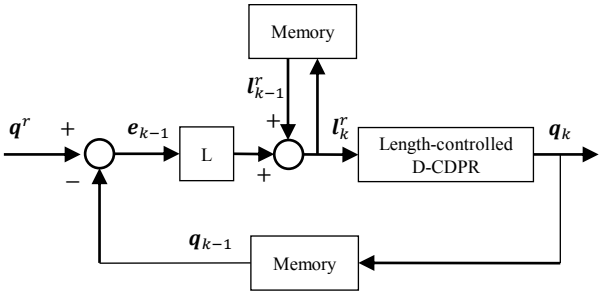

Fig. 3. Schematic diagram of linear ILC

As the mentioned sources of disturbance are usually in high frequency and low magnitude, applying a filter to the measured output can reduce the effect of the disturbance. In this experiment, a Gaussian filter is applied before feeding the output to the ILC law. The filtered output $\boldsymbol{q}_k$ is obtained from the reference EE pose $\boldsymbol{q}^r$ and the measured EE pose $\boldsymbol{q}^m_k$ as

$$\boldsymbol{q}_k = \boldsymbol{q}^r + G(\boldsymbol{q}^m_k - \boldsymbol{q}^r), \tag{8}$$

where G is the Gaussian filter.

C. Linear Iterative Learning Control

In this work, the tracking error induced from the varying attachment locations is reduced by ILC, which is a model-free learning-based controller [17]. By modifying the control input over repeating trajectories, ILC improves the tracking performance from iteration to iteration. The cable length input $\boldsymbol{l}^r_{k+1}$ of a simple first-order linear ILC law of the succeeding $(k+1)$ iteration is given by

$$\boldsymbol{l}^r_{k+1} = \boldsymbol{l}^r_k + \boldsymbol{L}\boldsymbol{e}_k, \tag{9}$$

where $\boldsymbol{e}_k \in \mathbf{R}^m$ is the tracking error between reference $\boldsymbol{q}^r$ and actual poses $\boldsymbol{q}_k$,

$$\boldsymbol{e}_k = \boldsymbol{q}^r - \boldsymbol{q}_k. \tag{10}$$

Hence $\boldsymbol{l}^r_{k+1}$ is dependent on the both previous input $\boldsymbol{l}^r_k$ and the previous tracking error $\boldsymbol{e}_k$, which are stored in the memory of the controller. Fig. 3 shows the block diagram of the linear ILC. The matrix $\boldsymbol{L} \in \mathbf{R}^{m\times n}$ is the learning gain.

To guarantee the convergence of the ILC, the chosen $\boldsymbol{L}$ has to fulfill the inequality

$$\|\boldsymbol{I} - \boldsymbol{L}\frac{\partial \boldsymbol{q}}{\partial \boldsymbol{l}}\| = \boldsymbol{\gamma} < 1, \tag{11}$$

where the operator $\|\cdot\|$ is the spectral norm of a matrix, i.e.

$$\|\boldsymbol{B}\| = \sqrt{\lambda_{\max}(\boldsymbol{B}^T\boldsymbol{B})}\ . \tag{12}$$

This is the necessary and sufficient condition for the controller to avoid producing divergent results [17]. In practice, there are non-repetitive disturbances and un-modelled system dynamics that could cause errors. To avoid instability, one could provide a buffer by setting the scalar γ smaller than 1. On the other hand, $\boldsymbol{L}$ also determines the convergent rate of the ILC. Hence, it is vital to obtain an appropriate learning gain $\boldsymbol{L}$.

IV. Selection of the Learning Matrix

In this section, it is shown that the Jacobian is a recommended candidate for the ILC learning gain. Hence, two types of learning gain based on the Jacobian matrix of the CDPR are presented. From (4), the relationship between actuation space and task space can be described by the Jacobian matrix. In the case of $m \leq n$, the change in EE pose (output) with respect to the cable length (input) can be formulated as

$$\frac{\partial \boldsymbol{q}}{\partial \boldsymbol{l}} = \boldsymbol{J}^+, \tag{13}$$

where $\boldsymbol{J}^+$ is the right pseudoinverse of $\boldsymbol{J}$,

$$\boldsymbol{J}\boldsymbol{J}^+ = \boldsymbol{I}. \tag{14}$$

By substitution, (11) can then be simplified as

$$\|\boldsymbol{I} - \boldsymbol{L}\boldsymbol{J}^+\| = \gamma < 1. \tag{15}$$

Hence the inequality (11) could be satisfied by setting $\boldsymbol{L}$ as the Jacobian matrix $\boldsymbol{J}$.

A. Scaled Jacobian Estimation with Constant Attachment Locations (JEC)

From (15), an intuitive choice of learning gain is the scaled Jacobian

$$\boldsymbol{L} = s\boldsymbol{J}, \tag{16}$$

where $s > 0$ is a scalar used to multiply the Jacobian. The inequality (11) becomes

$$\gamma = \|\boldsymbol{I} - s\boldsymbol{I}\| = |1 - s|. \tag{17}$$

To fulfill the inequality,

$$\gamma < 1 \implies 0 < s < 2. \tag{18}$$

When controlling the D-CDPR, the major source of system error is the deformable frame model. As the attachments are moving during operation, it is infeasible to obtain the Jacobian matrix accurately without having sufficient state feedback of the EE and the deforming frame. Hence it is recommended to take $s = 1$ to keep γ away from the limits to avoid overshooting and instability.

$$\gamma \approx 0, \tag{19}$$

With the nominal value of γ being 0, the convergence is most likely to be guaranteed. The Jacobian matrix $\boldsymbol{J}$ is estimated with constant attachment points $\hat{\boldsymbol{a}}_i$ assumption (JEC). Later in the experiment shows that the tracking error can still converge over iterations, despite the estimation errors caused by the frame deformation.

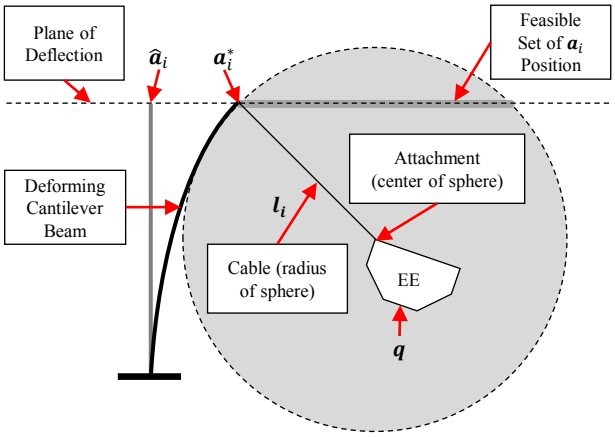

Fig. 4. Approximation of $\boldsymbol{a}_i^*$ position with JED

B. Jacobian Estimation with Deformable Frame Consideration (JED)

To obtain a more accurate Jacobian learning gain in ILC, a Jacobian estimation method is proposed. In the case of large frame deformation, the negative impacts on the previous JEC method could be significant. JED involves estimation of the cable attachment point motions, followed by computation of $\boldsymbol{J}$ from (1) and (5).

The frame attachment point at a particular time instance can be approximated using quadratically constrained quadratic programming (QCQP). This approach only requires the offline pose feedback of EE and cable length. The feasible set of $\boldsymbol{a}_i$ is first obtained by considering both the beam deflecting directions and sensor feedback.

As shown in Fig. 4, a plane perpendicular to the cantilever neutral axis is drawn to represent the potential deflection of the beam tip. This plane can be defined as a linear constraint

$$\boldsymbol{H}_i\boldsymbol{a}_i = \boldsymbol{d}_i \tag{20}$$

where $\boldsymbol{H}_i \in \mathbb{R}^{3\times3}$ and $\boldsymbol{d}_i \in \mathbb{R}^3$ are constants.

Another set of potential positions for $\boldsymbol{a}_i$ is obtained based on the EE pose and cable length feedback. This set is computed independently for every sampled time instance. Since cable can only carry tension but not compression, the cable length l_i represents the maximum distance between $\boldsymbol{a}_i$ and the attachment point on EE. As shown in Fig. 4, the set can be expressed as a sphere with the attachment point on EE as the center and l_i as the radius. The sphere can be defined as a convex constraint

$$\|\boldsymbol{c}_i(\boldsymbol{a}_i, \boldsymbol{q})\|_2^2 \leq l_i^2 \tag{21}$$

The overall feasible set of $\boldsymbol{a}_i$ can then be expressed as all the positions that satisfy (20) and (21) simultaneously. As cantilever beam stores elastic potential energy proportional to $\|\boldsymbol{a}_i - \hat{\boldsymbol{a}}_i\|_2^2$, the beam tip tends to $\hat{\boldsymbol{a}}_i$ in quasi-static motion. Therefore, the actual $\boldsymbol{a}_i^*$ at each sampled time instance can then be approximated by varying $\boldsymbol{a}_i$ to minimize the beam's elastic potential energy while fulfilling the constraints. Such optimization problem can be expressed in the QCQP form as

$$\begin{aligned} \boldsymbol{a}_i^* = \underset{\boldsymbol{a}_i}{\text{argmin}} \quad & \boldsymbol{a}_i^T\boldsymbol{Q}_0\boldsymbol{a}_i + \boldsymbol{p}_0^T\boldsymbol{a}_i \\ \text{s.t.} \quad & \boldsymbol{H}_i\boldsymbol{a}_i = \boldsymbol{d}_i \\ & \boldsymbol{a}_i^T\boldsymbol{Q}_1\boldsymbol{a}_i + \boldsymbol{p}_1^T\boldsymbol{a}_i \leq r_1, \end{aligned} \tag{22}$$

where

$$\boldsymbol{Q}_0 = \boldsymbol{Q}_1 = \boldsymbol{I} \succ 0 \tag{22a}$$

$$\boldsymbol{p}_0 = -2\hat{\boldsymbol{a}}_i \tag{22b}$$

$$\boldsymbol{p}_1 = -2(\boldsymbol{q}_p + \boldsymbol{R}(\boldsymbol{q}_r)\boldsymbol{b}_i) \tag{22c}$$

$$r_1 = l_i^2 - (\boldsymbol{q}_p + \boldsymbol{R}(\boldsymbol{q}_r)\boldsymbol{b}_i)^T(\boldsymbol{q}_p + \boldsymbol{R}(\boldsymbol{q}_r)\boldsymbol{b}_i). \tag{22d}$$

As $\boldsymbol{Q}_0$ and $\boldsymbol{Q}_1$ are positive definite, (22) is a convex QCQP problem [18]. It is reliable and efficient to solve such problem with various convex optimization solver [19], [20]. Furthermore, the formulation of (22) at different sampling time instances are independent, it is time efficient to obtain the $\boldsymbol{a}_i$ trajectory of an iteration by utilizing parallel processing.

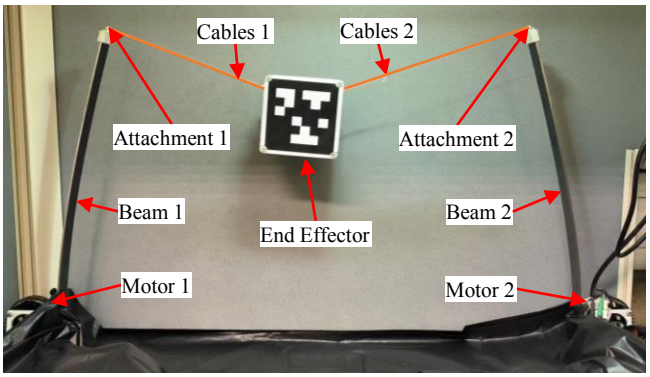

Fig. 5. Hardware setup of the planar point-mass suspended D-CDPR

V. Experiment

To evaluate the performance of the proposed ILC law with different learning gain matrices, a planar point-mass suspended D-CDPR (the robot) is used for the experiment.

A. Hardware Setup

As shown in Fig. 5, the robot has two vertical thin steel plates as the deformable frame. The cable attachment points are at the tips of the two identical plates, which have a height of 0.45 m and are 0.8 m apart. A 1.68 kg EE is suspended by two cables, where the cable length is controlled by two motors respectively.

An AprilTag [21] was attached to the EE to record the pose, as shown in Fig. 5. The robot were recorded at a frequency of 30 Hz by a camera, and the motion of the EE is calculated from the recordings afterward.

B. Experimental Result

Cable length control is used to maneuver the EE and track two different trajectories. The tested trajectories, named "rectangular" (Table I) and "L-shape" (Table II), are defined

TABLE I

FIXED POINTS (IN METERS) OF THE RECTANGULAR TRAJECTORY.

i	1	2	3	4	5	6	7	8
$\boldsymbol{q}_c^r(T_i)$	$\begin{bmatrix}0.40\\0.05\end{bmatrix}$	$\begin{bmatrix}0.40\\0.10\end{bmatrix}$	$\begin{bmatrix}0.65\\0.10\end{bmatrix}$	$\begin{bmatrix}0.65\\0.38\end{bmatrix}$	$\begin{bmatrix}0.15\\0.38\end{bmatrix}$	$\begin{bmatrix}0.15\\0.10\end{bmatrix}$	$\begin{bmatrix}0.40\\0.10\end{bmatrix}$	$\begin{bmatrix}0.40\\0.05\end{bmatrix}$
T_i	0s	1s	3s	5s	10s	12s	14s	15s

TABLE II

FIXED POINTS (IN METERS) OF THE L-SHAPE TRAJECTORY.

i	1	2	3	4	5	6	7
$\boldsymbol{q}_c^r(T_i)$	$\begin{bmatrix}0.40\\0.05\end{bmatrix}$	$\begin{bmatrix}0.40\\0.10\end{bmatrix}$	$\begin{bmatrix}0.65\\0.10\end{bmatrix}$	$\begin{bmatrix}0.65\\0.38\end{bmatrix}$	$\begin{bmatrix}0.65\\0.10\end{bmatrix}$	$\begin{bmatrix}0.40\\0.10\end{bmatrix}$	$\begin{bmatrix}0.40\\0.05\end{bmatrix}$
T_i	0s	1s	3s	5s	7s	9s	10s

as fixed points at various time instances T. The trajectory between each point is defined as

$$\begin{aligned}\boldsymbol{q}^r(t) &= \frac{t-T_i}{T_{i+1}-T_i}\left(\boldsymbol{q}^r(T_{i+1})-\boldsymbol{q}^r(T_i)\right)+\boldsymbol{q}^r(T_i)\\ \dot{\boldsymbol{q}}^r(t) &= \frac{\boldsymbol{q}^r(T_{i+1})-\boldsymbol{q}^r(T_i)}{T_{i+1}-T_i}\\ \ddot{\boldsymbol{q}}^r(t) &= \boldsymbol{0}.\end{aligned} \tag{23}$$

In iteration 0, the cable length input $\boldsymbol{l}_0^r$ is obtained by inverse kinematics with rigid frame assumption. ILC law is then applied to improve the performance in the follow-up iterations. ILC law with four different learning gain matrices, named "constant 1", "constant 2", "JEC" and "JED", are tested separately to compare their effectiveness.

As a comparison to the proposed approach, two constant learning gain

$$\boldsymbol{L}_{c1} = \begin{bmatrix}\frac{1}{\sqrt{2}} & -\frac{1}{\sqrt{2}}\\ -\frac{1}{\sqrt{2}} & -\frac{1}{\sqrt{2}}\end{bmatrix} \tag{24}$$

$$\boldsymbol{L}_{c2} = \begin{bmatrix}1 & 0\\ 0 & -1\end{bmatrix} \tag{25}$$

are tested. Constant 1 in (24) is manually tuned for tracking the rectangular trajectory, while Constant 2 in (25) is an arbitrary learning gain matrix. The JEC learning gain is obtained from (16) with $s = 1$. The JED learning gain is a modification of the JEC method where the frame attachment points are approximated from (22).

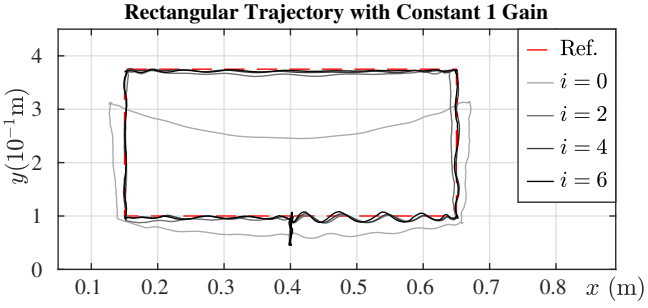

Fig. 6. Rectangular trajectory tracking with constant 1 learning gain.

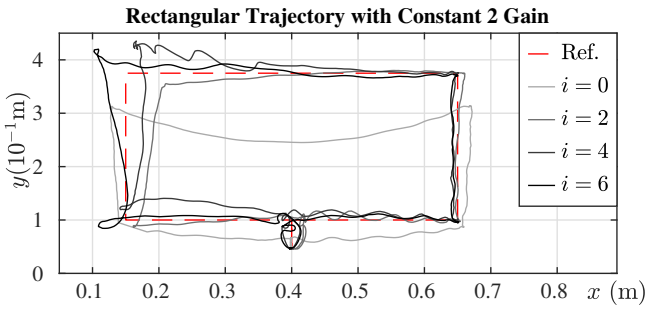

Fig. 7. Rectangular trajectory tracking with constant 2 learning gain.

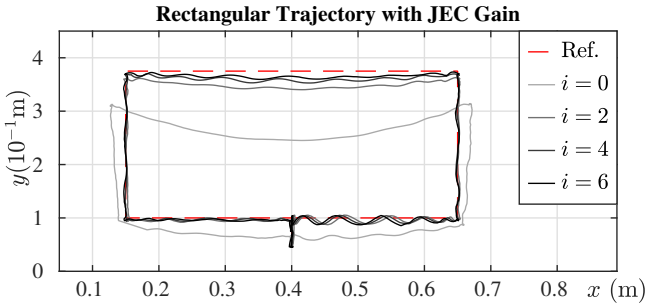

Fig. 8. Rectangular trajectory tracking with JEC learning gain.

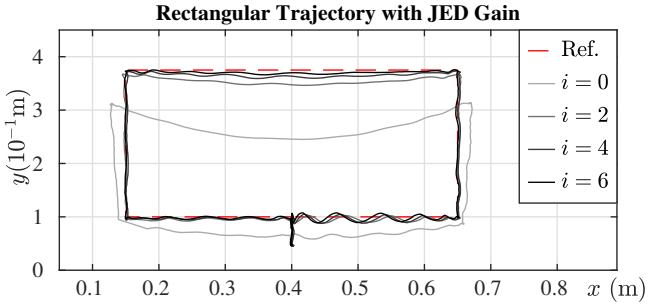

Fig. 9. Rectangular trajectory tracking with JED learning gain.

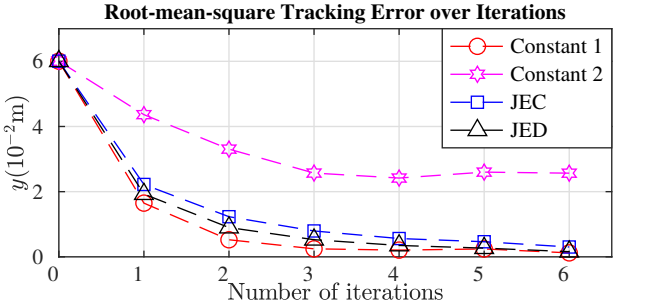

Fig. 10. Root-mean-square tracking errors of each iterations with different learning gains (rectangular trajectory)

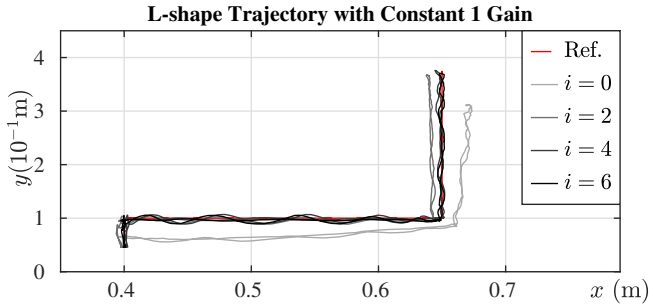

Fig. 11. L-shape trajectory tracking with constant 1 learning gain.

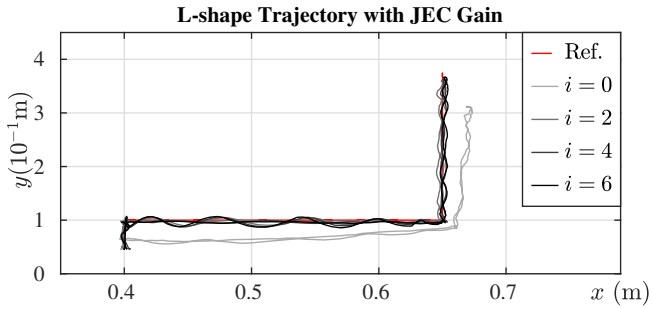

Fig. 12. L-shape trajectory tracking with JEC learning gain.

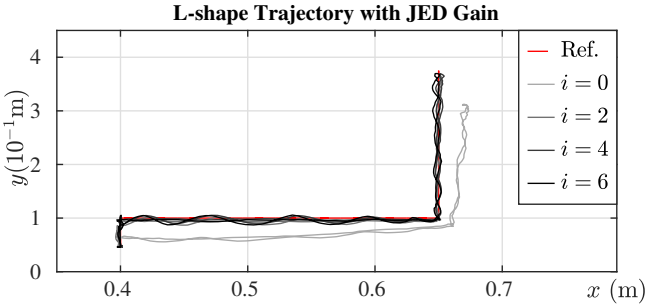

Fig. 13. L-shape trajectory tracking with JED learning gain.

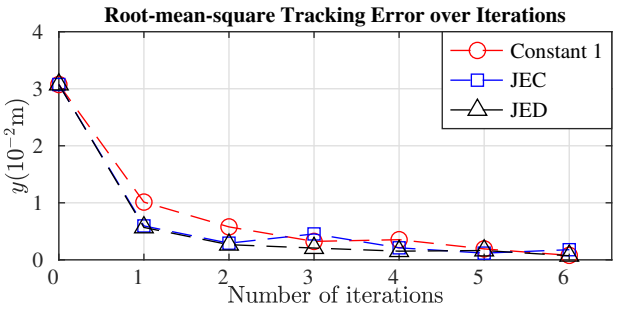

Fig. 14. Root-mean-square tracking errors of each iterations with different learning gains (L-shape trajectory).

1) Rectangular Trajectory: The measured EE trajectory $\boldsymbol{q}^m$ over iterations with different learning gain, including constant 1 (Fig. 6), constant 2 (Fig. 7), JEC (Fig. 8) and JED (Fig. 9), are shown respectively. All four types of learning gain are capable of improving the tracking performance significantly.

To compare the tracking performance between each iteration, the root-mean-square (RMS) of the filtered errors obtained from (8) and (10) is computed. The RMS errors over iterations with the three learning gains are shown in Fig. 10. As the frame deformation during manipulation is large, the motions of cable attachment points become crucial to the tracking performance. JED, which approximates the frame deformation, performs significantly better than JEC. The ILC with constant 1 learning gain has the fastest rate of convergence among the four options since the gain matrix (24) is manually tuned for this trajectory. Constant 2, which has particularly poor performance, shows the importance of manual tuning in constant learning gain. It also shows the significance of JEC and JED, as the Jacobian-based learning gain can provide a sufficiently high rate of convergence without manual tuning.

2) L-shape Trajectory: Similar to the rectangular trajectory, the L-shape trajectory is tested with three learning gains, constant 1 (Fig. 11), JEC (Fig. 12) and JED (Fig. 13) respectively. In this L-shape trajectory, the frame deformation is relatively small. Therefore, the performance of JED is similar to JEC as shown in Fig. 14. Different from the result obtained in rectangular trajectory tracking, the ILC with constant 1 learning gain performs worse than JED in this case. It is because the gain matrix (24) is not specialized for this L-shape trajectory. Manual tuning is required for better performance.

From the experimental results above, using a constant learning gain for D-CDPRs is feasible, but the performance greatly depends on the robot setup and the desired trajectory. Manual tuning of the gain matrix is required for each trajectory. Applying constant learning gain can save computation power but requires higher manual effort.

Jacobian-based learning gain performs consistently in different trajectories and the convergence can be guaranteed from (19). The performance of JED is particularly better than JEC when the frame deformation is large. In case of small deformation, the two approaches are similar and JEC will be the more computationally efficient option.

VI. Conclusion

In this paper, an ILC incorporated with cable length control is proposed for D-CDPRs. A novel JED approach is proposed to obtain better learning gain by approximating the deflection of the cable attachment points. This work is important to the application of D-CDPRs as it could achieve the desired performance without a dynamic model of the frame. Hardware experiment has shown promising results in the application of the proposed method. Prospective future works include modification on attachment points approximation and extension to nonlinear ILC law.

References

[1] S. Qian, B. Zi, W.-W. Shang, and Q.-S. Xu, "A review on cable-driven parallel robots," *Chinese Journal of Mechanical Engineering*, vol. 31, no. 1, pp. 1–11, 2018.

[2] X. Tang, "An overview of the development for cable-driven parallel manipulator," *Advances in Mechanical Engineering*, vol. 6, p. 823028, 2014.

[3] M. Zarebidoki, J. S. Dhupia, and W. Xu, "A review of cable-driven parallel robots: Typical configurations, analysis techniques, and control methods," *IEEE Robotics & Automation Magazine*, vol. 29, no. 3, pp. 89–106, 2022.
[4] A. N. F. Chan, W. Cheng, and D. Lau, "Deformable open-frame cable-driven parallel robots: Modeling, analysis and control," 2024.
[5] A. Pott, *Cable-Driven Parallel Robots: Theory and Application*. Springer, 2018, vol. 120.
[6] ——, "An algorithm for real-time forward kinematics of cable-driven parallel robots," in *Advances in Robot Kinematics: Motion in man and machine*. Springer, 2010, pp. 529–538.
[7] H.-S. Ahn, Y. Chen, and K. L. Moore, "Iterative learning control: Brief survey and categorization," *IEEE Transactions on Systems, Man, and Cybernetics, Part C (Applications and Reviews)*, vol. 37, no. 6, pp. 1099–1121, 2007.
[8] K. L. Moore, *Iterative learning control for deterministic systems*. New York: Springer-Verlag, 1993.
[9] D. Shen, "Iterative learning control with incomplete information: A survey," *IEEE/CAA Journal of Automatica Sinica*, vol. 5, no. 5, pp. 885–901, 2018.
[10] D. Bhattacharya, Y. P. Chan, S. Shang, Y. S. Chan, Y. Tan, and D. Lau, "Tri-space operational control of redundant multilink and hybrid cable-driven parallel robots using an iterative-learning-based reactive approach," *IEEE Transactions on Control Systems Technology*, vol. 31, no. 6, pp. 2465–2483, 2023.
[11] J.-X. Xu and Y. Tan, *Linear and nonlinear iterative learning control*. Springer, 2003, vol. 291.
[12] J.-X. Xu, "A survey on iterative learning control for nonlinear systems," *International Journal of Control*, vol. 84, no. 7, pp. 1275–1294, 2011.
[13] K. L. Moore, Y. Chen, and H.-S. Ahn, "Iterative learning control: A tutorial and big picture view," in *Proceedings of the 45th IEEE Conference on Decision and Control*. IEEE, 2006, pp. 2352–2357.
[14] Z. Li, W. Chen, J. Zhang, and S. Bai, "Design and control of a 4-dof cable-driven arm rehabilitation robot (CARR-4)," in *2017 IEEE International Conference on Cybernetics and Intelligent Systems (CIS) and IEEE Conference on Robotics, Automation and Mechatronics (RAM)*. IEEE, 2017, pp. 581–586.
[15] S. Liu, D. Meng, L. Cheng, and M. Chen, "An iterative learning controller for a cable-driven hand rehabilitation robot," in *IECON 2017-43rd Annual Conference of the IEEE Industrial Electronics Society*. IEEE, 2017, pp. 5701–5706.
[16] J. Peng, H. Wu, and D. Lau, "Operational space iterative learning control of coupled active/passive multilink cable-driven hyper-redundant robots," *Journal of Mechanisms and Robotics*, vol. 15, no. 1, p. 011013, 2023.
[17] D. A. Bristow, M. Tharayil, and A. G. Alleyne, "A survey of iterative learning control," *IEEE control systems magazine*, vol. 26, no. 3, pp. 96–114, 2006.
[18] X. Bao, N. V. Sahinidis, and M. Tawarmalani, "Semidefinite relaxations for quadratically constrained quadratic programming: A review and comparisons," *Mathematical programming*, vol. 129, pp. 129–157, 2011.
[19] S. P. Boyd and L. Vandenberghe, *Convex optimization*. Cambridge university press, 2004.
[20] D. Bertsekas, *Convex optimization algorithms*. Athena Scientific, 2015.
[21] E. Olson, "Apriltag: A robust and flexible visual fiducial system," in *2011 IEEE International Conference on Robotics and Automation*. IEEE, 2011, pp. 3400–3407.